

 Open access • Journal Article • DOI:10.1007/BF01559588

Mass and lifetime limits on new long-lived particles in 300 gev/c pi - interactions

— [Source link](#) 

J. Badier, C. Bemporad, A.M. Cnops, G. Giannini ...+14 more authors




Institutions: École Polytechnique, University of Pisa, Collège de France, CERN

Published on: 07 Feb 1986 - European Physical Journal C (Springer-Verlag)

Topics: Pion, Elementary particle and Range (particle radiation)

Related papers:

- [Search for neutral heavy leptons produced in Z decays](#)
- [Search for Heavy Neutrino Decays in the {BEBC} Beam Dump Experiment](#)
- [Further limits on heavy neutrino couplings](#)
- [The Search for Heavy Majorana Neutrinos](#)
- [\$\mu \rightarrow e \gamma\$ at a rate of one out of 109 muon decays?](#)

Share this paper:    

View more about this paper here: <https://typeset.io/papers/mass-and-lifetime-limits-on-new-long-lived-particles-in-300-4jhqlptqx2>



MASS AND LIFETIME LIMITS ON NEW LONG-LIVED PARTICLES
IN 300 GeV/c π^- INTERACTIONS

NA3 Collaboration

CEN, Saclay¹- CERN, Geneva²- Collège de France, Paris³-
Ecole Polytechnique, Palaiseau⁴- Lab. de l'Accélérateur Linéaire, Orsay⁵-
Università di Pisa and INFN, Pisa⁶

J. Badier⁴, C. Bemporad⁶, J. Boucrot⁵, O. Callot⁵,
P. Charpentier¹, A.M. Cnops⁶, M. Crozon³, P. Delpierre³,
J.F. Detoef¹, G.R. Giannini⁶, R. Hammarström², P. Lariccia⁶, R. Lorenzi²,
J. Mas³, A. Michelini², A. Tilquin²⁻³ and J.K. Walker^{5*}.

ABSTRACT

A sensitive search has been done for the production of new long-lived and penetrating particles by 300 GeV/c negative pions. No new state - decaying into at least two charged known particles - has been detected with mass above 1 GeV/c² and lifetime in the range $5 \cdot 10^{-11}$ s to $5 \cdot 10^{-7}$ s. We give upper limits on production cross sections, and consequences on the existence of heavy "axion-like" particles, heavy neutrinos and super-symmetric particles. In particular, this experiment excludes the existence of light gluinos with lifetime in the range $5 \cdot 10^{-11}$ to 10^{-8} s: this closes the last "window of opportunity" for gluinos with $M < 2$ GeV/c² and lifetime measurable in particle physics experiments.

(Submitted to Zeitschrift für Physik C)

(*) Permanent address: Fermilab, P.O. Box 500, Batavia, IL 60510 (USA)

1. INTRODUCTION: PHYSICS MOTIVATIONS

A search for new and penetrating long-lived particles has been performed at CERN SPS, using the NA3 spectrometer. The experiment was motivated by the fact that no direct sensitive search for new neutral states has been done in the lifetime range 10^{-10} to 10^{-8} s, thus leaving open a window for light supersymmetric particles as gluinos; this was pointed out by Dawson et al. [1], see also ref. 2.

The present experiment uses a beam of 300 GeV/c π^- incident on a dump 2m long. Negative pions are expected to be more efficient to produce heavy states than protons at the same energy, due to the possibility of quark-antiquark annihilations (for instance, T production is ~ 100 times larger in π^- interactions than in p interactions at 300 GeV/c, ref. 3). Higher cross-sections for production of heavy states are also expected in π^- interactions through gluon-gluon fusion, due to the gluon distribution in the pion, which is much harder than in the proton [4].

In the present experiment, the beam dump is followed by a decay region 2m long, the decay products being analyzed in a large acceptance spectrometer. The apparatus is able to make a good identification of leptons and hadrons in the final state; it is sensitive to the decay of neutral or charged particles with lifetimes between $5 \cdot 10^{-11}$ and $5 \cdot 10^{-7}$ s, requiring that at least two charged particles are present in the final state.

Therefore, this experiment is able to detect directly any state, within the above lifetime limits, with decay states like e^+e^- , $\mu^+\mu^-$, $e\mu$, $\pi\mu$, $\pi^+\pi^-$ (or n charged pions, with $n \geq 2$), and also K^\pm , K_S^0 or protons in the final state.

In Sect. 2, we describe the experimental set-up and data taking conditions, and the observed particle spectra in various leptonic and hadronic channels. In Sect. 3, we determine the acceptance for the observed channels, and the corresponding cross-section limits. Finally, we give in Sect. 4 the consequences of these limits on several predictions concerning expected "new" particles such as axion-like bosons, heavy neutrinos, and supersymmetric particles like gluinos.

2. EXPERIMENTAL SET-UP AND DATA ANALYSIS

2.1 The experimental set-up

We use the NA3 spectrometer in a beam dump configuration (which is described in detail in ref. 5), with the following modifications (fig. 1):

- The incoming beam is a secondary 300 GeV/c π^- beam, with average intensities of $9 \cdot 10^6$ to $1.7 \cdot 10^7$ particles per burst, depending on the dump length. The beam intensity is determined by the maximum trigger rate compatible with the acquisition system.
- The hadron iron absorber, with an axial conical tungsten plug of 20 mrad aperture, is 2m long for one half of the data, 2.2m for the remaining half. No target is mounted in front of the absorber (fig. 1).
- The forward arm of the spectrometer (between the dump and the magnet) is modified with respect to the description of ref. 5, in order to provide a decay path in a cylindrical vacuum tank, 2m long and 1.5m in diameter, with thin aluminium windows 1mm thick. This allows the suppression of interactions coming from punch-through particles, which may simulate in-flight decays. Two hodoscopes, T1 and T2, are mounted at each end of the vacuum tank for trigger purposes; they are designed [6] to avoid random coincidences from slow neutrons generated in the dump.

This set-up has a powerful particle identification, performed in the following way:

- i) muons above 2 GeV/c are identified by the energy deposited in the third section of the electromagnetic calorimeter, and by the hodoscope T3 located behind an iron filter 1.8 m thick (fig. 1);
- ii) electrons and photons are identified in the two first sections of the electromagnetic calorimeter;
- iii) a $\pi/K/p$ discrimination is possible in the multicell Čerenkov counters C_2 (24 cells) and C_3 (36 cells) [7]. Charged kaons are identified above 11 GeV/c and protons (or antiprotons) above 15 GeV/c.

2.2 Trigger and data reduction

The trigger requirements define two categories of events, corresponding to the decay of neutral (charged) particles in the vacuum tank. These requirements are:

- an incoming beam particle;
- zero (one) charged particle behind the dump and before the vacuum tank;
- at least 2 (3) charged particles in the spectrometer (in chamber CH3).

The total data collected correspond to $6.4 \cdot 10^6$ recorded second level triggers, obtained by filtering $18.5 \cdot 10^6$ first level triggers. The filtering is performed by a hardware processor and a 168/E emulator providing together on-line pattern recognition.

The data correspond to an integrated luminosity $L = 6.9 \pm 0.7 \cdot 10^{37} \text{ cm}^{-2}$.

2.3 Data analysis and event reconstruction

The events recorded on tape consisted essentially of decays of known strange particles produced inside the dump, and also of interactions by punch-through hadrons in the counters or in the walls of the vacuum tank.

The off-line event filtering proceeds through the following steps and conditions:

- Consistency is required between the reconstructed tracks multiplicity, the trigger conditions and the multiplicity recorded by the T1, and by the CH1 and CH2 chambers. This rejects about 90% of charged triggers and 60% of neutral triggers.
- It requires the presence of at least a two-prong vertex for neutral triggers, and a three-prong vertex for charged triggers; afterwards a search is made for known decay channels (Table I). A decay compatible with a known particle can be used in further vertex finding. Each particle from a decay vertex is tested against the hypotheses of being a lepton, a charged kaon or a proton. If all these hypotheses fail, the particle is considered to be a charged pion.
- It requires only one ingoing particle; this means no unassociated tracks and only one "tree" of vertices.

- The final analysis includes events with a vertex inside a fiducial decay path 1.6 m long, starting 20 cm from the entrance window of the vacuum tank and ending 20 cm in front of the exist window. The choice of these limits is suggested by the reconstructed vertex spatial resolution, which is 3.7 cm for a 600 MeV/c² state decaying into 2 charged particles, and less than 1 cm for decaying states above 2 GeV/c². This cut rejects about 50% of good triggers, coming from interactions in the hodoscopes or in the walls of the vacuum tank.

The total final statistics is about 260 000 events. Almost all of them are decays of known strange particles, mostly $K_S^0 \rightarrow \pi^+\pi^-$. Table I gives the statistics on identified decay channels, and the mean reconstructed mass, in good agreement with the world average [8]. More details on the properties of punch-through charged or neutral particles in this experiment may be found in ref. 9.

2.4 Mass spectra

We can give now the invariant mass spectra obtained in various channels with identified particles in the final state. The main background to a search for new particles comes essentially from the $K_S^0 \rightarrow \pi^+\pi^-$ decays: they may give, from subsequent π decay, $\pi\mu$ or $\mu^+\mu^-$ low mass final states; they may also, from π scattering in the materials behind the fiducial volume, give a reconstructed $\pi^+\pi^-$ mass above the K_S^0 mass. K_L^0 decays also contribute to backgrounds in $\pi^+\pi^-$, πe and $\pi\mu$ channels, below the K mass due to the missing neutral particle.

In the following, we deal with two sets of mass spectra. The first set is obtained without any further cut, and may be used to give limits on final states with missing neutral particles. The second set concerns uniquely the search for exclusive two-body charged final states: a large fraction of events with scattering of the decay products, or with missing particles, may be eliminated by requesting that the transverse momentum P_{out} , perpendicular to the plane containing the vertex and the beam line, should be lower than 200 MeV/c. This eliminates only 9% of reconstructed K_S^0 events, and almost all events with $M(\pi^+\pi^-) > 600$ MeV/c².

Some mass spectra of these above sets are displayed in figs. 2 and 3; statistics and highest mass value in various channels are given in Table II.

From inspection of mass spectra and Table II we conclude that no signal of any new particle decaying in standard known particles is seen in any channel. We will now give the corresponding cross-section limits for various final states.

3. ACCEPTANCE AND-CROSS SECTION LIMITS

3.1 Acceptance calculations

The acceptance of the experiment apparatus to a produced particle with mass M , decaying with a lifetime τ into a given final state, is determined from a complete Monte-Carlo simulation.

The generated events are processed through the simulation program of the apparatus, using the CERN Geant package [10], and analyzed like real events through the same chain of reconstruction programs.

The acceptance is determined under the following assumptions:

- (i) the decay probability inside the vacuum tank must be reasonably large: we have generated particles with lifetime $5 \cdot 10^{-11} \text{s} < \tau < 5 \cdot 10^{-7} \text{s}$ which corresponds (for particles with $x_F = 0$) to decay probabilities greater than 10^{-4} and at most $\sim 18\%$. In what follows the "acceptance" will always include this decay probability;
- (ii) the particle does not interact in the beam dump. The problem of these interactions will be treated in Sect. 3;
- (iii) the particle is produced with an invariant cross-section

$$E \frac{d^3\sigma}{dp^3} \propto (1-|x_F|)^4 \exp(-1.1 p_T^2) \quad (3.1)$$

This "central" cross-section is compatible with the known behaviour of heavy flavour hadroproduction [e.g. ref. 11]. It may be not realistic for the production of low-mass states (below $\sim 1.5 \text{ GeV}/c^2$) but, due to the excellent geometrical acceptance of the present set-up the p_T dependence is almost without effect. The precise x_F dependence of the cross-section is not a fundamental problem; we have checked that a $(1-|x_F|)^7$ behaviour [ref. 12] gives at most 20% difference in the acceptance with respect to (3.1); a completely flat x_F distribution (quite unreasonable for heavy state production) may give an acceptance 1.6 times lower than (3.1) above $1.5 \text{ GeV}/c^2$, and a factor ~ 3 below $500 \text{ MeV}/c^2$.

The total acceptance (taking into account the decay probability in the vacuum tank and the reconstruction efficiency) is 12% in the most favourable case ($\tau = 10^{-9}$ s and $X^0 \rightarrow \pi^+\pi^-$ with $M(X) > 2 \text{ GeV}/c^2$). In the following, we give limits on the cross-sections only if the total acceptance is greater than 0.01%.

3.2 Cross-section limits

Some examples of the resulting 90% C.L. limits on production cross-section times branching ratio, σB per nucleon, are displayed in Figs. 4 and 5. The following points must be noted:

- these limits are valid only for particles not interacting with nuclear matter in the dump; if particles with interaction cross sections are considered, the limits must be multiplied by the factors given in Table III; the method used to estimate these factors is described in the Appendix;
- we assume a linear A-dependence of the cross-section with respect to the atomic number A of the target nucleus; if a dependence like $A^{0.75}$ is taken (as claimed by some experiments for charm production, ref. 13) one must multiply all cross-sections limits by a factor 3.7;
- these 90% C.L. upper limits may be raised by a factor ~ 2 to 3 if the production mechanism is not a central one but a diffractive one;
- as the hypothetical "new" particles may be produced at any step of the hadron shower development inside the dump, the limits quoted above may be substantially decreased if one takes into account the contribution of all secondary interactions in the shower.

3.3 Summary and Comparison with Previous Experiments

To summarize the above results we can say that the present experiment sets 90% C.L. limits on the production cross-section of new particles of mass M, times the branching ratio B:

$$\begin{aligned} B\sigma &\leq 2 \text{ picobarns/nucleon} && \text{for } M > 2. \text{ GeV}/c^2 \text{ and } 5 \cdot 10^{-10} < \tau < 10^{-8} \text{ s} \\ B\sigma &\leq 10 \text{ pb/nucleon} && \text{for } M > 1.5 \text{ GeV}/c^2 \text{ and } 10^{-10} < \tau < 10^{-8} \text{ s} \end{aligned}$$

Limits around 100pb/nucleon are obtained for low-mass e^+e^- final states, and for all states with lifetimes from 10^{-8} to $5 \cdot 10^{-7}$ s.

These limits are not very sensitive to the production mechanism; but they apply only to not interacting particles. If the hypothetical new particle may interact with the nuclear matter in the dump with a sizeable cross-section σ_0 , the upper limits given in all this section must be multiplied by a factor, F , which grows very quickly with σ_0 and is given in Table III.

The comparison with previous experiments is not easy since these have been done in very different conditions, almost all of them with an extremely small geometrical acceptance.

In the lifetime range $10^{-11} < \tau < 10^{-8}$ s, results have been given either by bubble chamber experiments or by measurements in hyperon beams. Bubble chambers have an excellent geometrical acceptance, but limited statistics; the upper limits on either neutral or charged states above $0.5 \text{ GeV}/c^2$ are around $1 \text{ } \mu\text{b}/\text{nucleon}$ [14]; these limits are valid even for strongly interacting particles. For not interacting particles, our limits are 5 to 6 orders of magnitude lower. Measurements in hyperon beams give limits only on charged particles, and have a sensitivity peaking around the typical hyperon lifetime ($\sim 10^{-10}$ s). Limits are given for masses between 1 and $2 \text{ GeV}/c^2$ [15] or 2 and $10 \text{ GeV}/c^2$ [16]. The best limits given ($X^-/\pi^- < 6 \cdot 10^{-8}$) are ~ 5 orders of magnitude greater than ours, for not interacting particles. A recent measurement [17] gives limits $X^-/\pi^- < 10^{-10}$ for charged particles with masses between 4 and $12 \text{ GeV}/c^2$ and lifetimes above $3 \cdot 10^{-9}$ s; these limits are valid for strongly interacting particles.

For $10^{-8} < \tau < 5 \cdot 10^{-7}$ s, our acceptance drops rapidly (the cut at $\tau = 5 \cdot 10^{-7}$ s corresponds roughly to an acceptance lower than 0.01%). In spite of this, our limits compare well with previous experiments with beam dumps (which all have extremely small geometrical acceptance, typically some microsteradians) in this lifetime range. The limits of ref. 18 vary from 25 nanobarns/nucleon to 25 picobarns/nucleon for neutral states with masses from 3 to $12 \text{ GeV}/c^2$ and $\tau > 10^{-7}$ s. The limits of ref. 19 concern only charged states with $\tau > 5 \cdot 10^{-8}$ s and masses from 1 to $7 \text{ GeV}/c^2$; they are comparable to ours but with very limited acceptance and therefore possible model dependence.

Other experiments, without beam dumps, have given results for charged particles only. A Fermilab experiment [20] gives a limit $\sigma < 20$ picobarns/nucleon for $4.5 < M < 6 \text{ GeV}/c^2$ and $\tau > 5 \cdot 10^{-8} \text{ s}$. Two ISR experiments at $\sqrt{s} = 53 \text{ GeV}$ [21], for $\tau > 10^{-8} \text{ s}$ and $2 < M < 20 \text{ GeV}/c^2$, give upper limits which are not very stringent ($X^-/\pi^- < 10^{-8}$), but independent of hypotheses on interaction cross-sections.

To summarize this discussion, the present results considerably improve (2 to 5 orders of magnitude) the previous limits on the hadroproduction of not interacting heavy new particles in the lifetime range $5 \cdot 10^{-11}$ to 10^{-8} s ; even allowing for interaction cross-section from 1 to 5 millibarns gives a significant improvement on the limits available so far. For longer lifetimes ($\tau > 10^{-8}$ to $5 \cdot 10^{-7} \text{ s}$) the present results overlap, with comparable sensitivities, with the best previously published limits.

4. CONSEQUENCES ON HYPOTHETICAL NEW PARTICLES

In this section we will try to discuss the consequences of the cross-section limits obtained in section 3, on the physical parameters of several hypothetical long-lived states predicted by various models. The results obtained in this section are therefore non-exhaustive and, in general, model-dependent.

4.1 Consequences on "Axion-like" Particle Production

We now discuss the consequences of the cross-section limits given in Fig. 4 for the production of "axion-like" bosons, loosely interacting with matter, as suggested by J. Bjorken [22]. We do not consider in the following axions decaying into a $\gamma\gamma$ pair, since the present experiment cannot give results on this final state. The axion-like bosons X^0 of mass M_X are supposed to decay into an e^+e^- pair if $1 \text{ MeV}/c^2 < M_X < 210 \text{ MeV}/c^2$, into a $\mu^+\mu^-$ pair if $210 \text{ MeV}/c^2 < M_X < \sim 1 \text{ GeV}/c^2$, and into a quark antiquark pair $q\bar{q}$ for $M_X > \sim 1 \text{ GeV}/c^2$ (giving therefore at least a $\pi^+\pi^-$ pair, or two hadron jets). Their decay rate into 2 fermions of mass m is given by the expression [23]:

$$\Gamma = \frac{m^2 \sqrt{M_x^2 - 4m^2}}{8\pi F_x^2} \quad (4.1)$$

F_x is the decay constant of the axion-like boson, usually expressed in GeV and related to the π^0 decay constant F_{π^0} by the relation:

$$\frac{\sigma(X^0)}{\sigma(\pi^0)} = \left(\frac{F_{\pi^0}}{F_x} \right)^2 \quad \text{with } F_{\pi^0} = 0.094 \text{ GeV} \quad (4.2)$$

Therefore the axion-like boson is characterized by the quantities F_x and M_x ; from relations (4.1) and (4.2) and from the upper limits on $\sigma(X^0)$ derived in section 3.2 one can exclude the existence of axion-like particles in given regions of the F_x, M_x plane. The result is displayed in Fig. 6, where other limits coming from previous experiments have been taken from ref. 24.

The limits obtained in the present experiment in the e^+e^- final state overlap partially with a region already excluded by the CHARM beam dump experiment [24] and partially with a region excluded by limits on J/ψ [25] and Υ [26] radiative decays. Therefore we confirm, by a different experimental approach, the non-existence of axion-like bosons in the quoted M_x, F_x region. It is worth noting that, in order to exclude axions decaying into $\mu^+\mu^-$ in the lifetime range accessible to the present experiment (which would have excluded the as yet unexplored region $0.2 < M_x < 1 \text{ GeV}/c^2$, $2 \cdot 10^4 < F_x < 2 \cdot 10^5$) would have required with our set-up a luminosity ~ 1000 times higher than what has been achieved. The same remark is valid for the $\pi^+\pi^-$ final state.

4.2 Consequences on the Existence of Gluinos

As the present experiment was conceived essentially as a gluino search and the experimental results are new and interesting, we will give more details on this point.

4.2.1 General Outlook

The cross-section limits of Fig. 5c and the non-observation of multiparticle hadronic decays, may be translated into limits on the existence of gluinos. These hypothetical particles are fermions, partners of gluons in

supersymmetry [27], a theory which has raised considerable interest in particle physics for many years. Gluinos are expected to be copiously produced in hadron-hadron collisions, but as there is no theoretical prejudice on their mass, it is important to exclude experimentally their existence even for low-masses. In 1984, the claim for "monojet" events in the UA1 experiment at the Sp \bar{p} S collider [28] raised a considerable interest since these events could be interpreted in some schemes by heavy gluinos [29] ($M_{\tilde{g}} \sim 40-60 \text{ GeV}/c^2$) and in others by light gluinos [30] ($M_{\tilde{g}} < 3 \text{ GeV}/c^2$); in 1985 this "signal" has washed off and is considered as compatible with much more conventional explanations [31].

Therefore all experimental results which may exclude the existence of gluinos in a given domain remain important. To perform the subsequent analysis, we have followed as close as possible the assumptions made by previous experiments on the same subject, in order to give results which may be compared directly.

4.2.2 How to find gluinos in hadroproduction?

Gluinos are neutral fermions which are expected to be principally pair-produced, in hadronic collisions, from gluon-gluon fusion ($gg \rightarrow \tilde{g}\tilde{g}$) or from quark anti-quark annihilation ($q\bar{q} \rightarrow \tilde{g}\tilde{g}$) [1,2]. They are not expected to be detected as "bare" particles, but confined in so-called "R-hadrons" [32], which may be either neutral or charged states. The masses of these states have been estimated for either R-mesons ($\tilde{g} q\bar{q}$ states, see, for instance, ref. 33) or R-baryons ($\tilde{g} qqq$ states, see ref. 34) and are not very different from the gluino mass, the difference being significant only for $M_{\tilde{g}} < 1 \text{ GeV}/c^2$; this point is discussed in detail for instance in ref. 2, Section 3.4. In the following, we will always consider that $M_{\tilde{g}} \approx \text{mass of the R-hadron}$.

4.2.3 Gluino cross-section production:

The elementary gluino production cross-section has been estimated by several authors [1,2,35,36], from gluon-gluon fusion or quark-antiquark annihilation. The resulting cross-sections predicted from real particles have been given only for pp or p \bar{p} collisions. The numerical values are important; at the energy of the present experiment ($\sqrt{s} = 23.7 \text{ GeV}$) from the values given in ref. 36 we have for gluino production in p \bar{p} collisions $\sigma \sim 10 \mu\text{b}$ for $M_{\tilde{g}} = 2 \text{ GeV}/c^2$, $\sigma \approx 4 \text{ nb}$ for $M_{\tilde{g}} = 5 \text{ GeV}/c^2$.

The authors of ref. 36 point out a very important point: the calculated cross-section for $gg \rightarrow \tilde{g}\tilde{g}$ in p-p collisions is very sensitive to the x_F behaviour of the proton gluon structure function (the cross-section is ~ 10 times larger, for $M \sim 2 \text{ GeV}/c^2$, from an $(1-x)^5$ behaviour, with respect to an $(1-x)^6$ behaviour, and this factor increases rapidly with M). As we are dealing with incoming pions which have a much harder gluon structure function, the $gg \rightarrow \tilde{g}\tilde{g}$ cross-section should be significantly higher from incident π^- than from p at the same energy. Moreover, $q\bar{q}$ annihilation contribute to gluino production at the same level than gluon-gluon fusion (ref. 36, Fig. 3). Therefore it seems to us that, at fixed \sqrt{s} , π^-p interactions are by far the best place to detect "light" gluinos.

However, as we do not have a theoretical prediction of gg production from incident π^- , we have chosen the following hypotheses (which were in general already taken by previous experiments looking for gluino production in hadron collisions, refs. 37 to 39):

- gluino production has the same behaviour as heavy quark hadroproduction, at the same energy, multiplied by the color factor $C = 81/7$ which accounts for the color octet nature of the gluino [ref. 37];
- the mass dependence of the cross section follows a power law $\sigma \propto M^{-n}$. The value $n = 7$ accounts equally well for hadronic production of heavy flavours (charm, ref. 12 and beauty, ref. 40) as for hidden flavour production (J/ψ , ref. 4 and T , ref. 41). This dependence is taken for $M_{\tilde{g}} > M_D$; it also reproduces well the mass-dependence of the $gg \rightarrow \tilde{g}\tilde{g}$ cross-section of ref. 36 at high $M_{\tilde{g}}$ mass. For $M_{\tilde{g}} < M_D$, we have chosen quite arbitrarily a much smoother dependence ($n = 2$), which reproduces reasonably ref. 36 for masses around $1 \text{ GeV}/c^2$.

We have considered the same charm-compatible X_F and P_T dependence as in section 3.2, i.e. proportional to $(1-|x_F|)^4 \exp(-p_T^2)$.

To summarize, we take the following expressions:

$$\sigma(\pi^-p \rightarrow \tilde{g}\tilde{g}) = 81/7 \sigma(\pi^-p \rightarrow D\bar{D}) (M_D/M_{\tilde{g}})^n \quad (4.3)$$

$$\begin{aligned} \text{with } n &= 7 \text{ for } M_{\tilde{g}} > M_D \\ n &= 2 \text{ for } M_{\tilde{g}} < M_D \end{aligned}$$

and $\sigma(\pi^- p \rightarrow D\bar{D}) = 20 \text{ } \mu\text{b}$ for incident 300 GeV/c π^- , from interpolation of the results of ref. 12 at 360 GeV/c.

As we are producing particles on heavy tungsten nuclei and not on free protons, we take conservatively a nuclear-dependence of the cross-section

$$\sigma(A) = \sigma(p) A^{0.75}$$

as given for charm hadroproduction by ref. 13.

4.2.4 Gluino Lifetime and Decay Products

The dominant decay of gluinos [2] is expected to be mediated by the scalar s quark of mass $M_{\tilde{q}}$, giving a decay $\tilde{g} \rightarrow q\bar{q}\tilde{\gamma}$ where q and \bar{q} are ordinary light quarks and $\tilde{\gamma}$ is the photino (supersymmetric partner of the photon). Other possible decays such as $\tilde{g} \rightarrow g\tilde{\gamma}$ or $\tilde{g} \rightarrow gG$ (where G is a "goldstino") are expected to be negligible [27].

For the $\tilde{g} \rightarrow q\bar{q}\tilde{\gamma}$ decay, the gluino lifetime may be calculated assuming that $M_{\tilde{g}} \gg M_q$ [1,2]

$$\tau = \frac{48\pi}{\alpha_e \alpha_s e_q^2} = \frac{M_{\tilde{q}}^4}{M_{\tilde{g}}^5} \quad (4.4)$$

After summation over light quarks (u,d,s) one obtains numerical values which may differ by a factor ~ 2 according to the value given to α_s :

$$\tau = C \frac{M_{\tilde{q}}^4}{M_{\tilde{g}}^5}$$

If $M_{\tilde{q}}$ and $M_{\tilde{g}}$ are expressed in GeV/c², the numerical values of C found in the litterature vary from $C = 4 \cdot 10^{-20}$ [1] to $C = 10^{-19}$ [37]. We will take in the following the intermediate value $C = 7.5 \cdot 10^{-20}$, but the final results do not depend sensitively on this precise value.

The final state corresponding to $\tilde{g} \rightarrow q\bar{q}\tilde{\gamma}$ consists therefore of an undetectable escaping photino, and of hadrons. As gluinos are embedded in R-hadrons, the decay final state is more likely a bunch of hadrons corresponding to the "dressing" of at least 4 quarks. We will assume in the following that our apparatus is able to see all these hadronic states (i.e. entirely neutral states are quite unlikely).

A last problem remains, which concerns the photino mass $M_{\tilde{\gamma}}$. In most "reasonable" supersymmetric models one admits that $M_{\tilde{\gamma}} \sim M_{\tilde{g}}/6$ or $M_{\tilde{g}}/7$ [27]. This is the hypothesis adopted in the analysis of previous experiments [37 to 39] and in order to compare with them, we have also adopted $M_{\tilde{\gamma}} \sim M_{\tilde{g}}/6$. However, there exist models [30] in which $M_{\tilde{\gamma}}$ is very close to $M_{\tilde{g}}$. This would alter considerably the results which will be presented in the following, since the resulting acceptance for a given $M_{\tilde{g}}$ would be much smaller.

4.2.5 Limits Coming from the Present Experiment

We have generated gluinos according to all the hypotheses discussed above, with mass ranging from 1 to 12 GeV/c² and lifetimes from $5 \cdot 10^{-11}$ to $5 \cdot 10^{-7}$ s. Comparing the expected number of events with the experimental distributions obtained (we do not consider events with $M(\pi^+\pi^-) < 0.8$ GeV/c² or $M(3\pi) < 0.8$ GeV/c² in order to avoid contaminations from K decays) we exclude the existence of gluinos inside the 90% C.L. contours drawn in Fig. 7. The different contours correspond to various values of the R-hadron interaction cross-section in the nuclear matter of the dump. It is worth noting that refs. 33 and 35 consider that the R-hadron interaction cross-section should be of the order of a few millibarns, which is comparable to what is known for other heavy states (e.g. 2mb/nucleon for the J/ψ).

If we take, for instance, $\sigma_0 = 5$ mb we may tentatively conclude that we exclude charged or neutral R-hadrons with $1 < M < 7$ GeV/c² with lifetimes $10^{-10} < \tau < 10^{-7}$ s, corresponding to squark masses in the range 120 GeV to ~ 6 TeV. The corresponding mass limits on gluinos depend on the mass relation between gluinos and R-hadrons.

4.2.6 Comparison with Previous Experiments

In Fig. 7 we have compiled the limits given by various previous experiments. The present work fills the last "window of opportunity", which was pointed out by the authors of refs. 1 and 2 for low-mass gluinos. We want to stress the following comments:

- (i) the limits obtained by neutrino beam-dump experiments [37-39] depend on a cascade of assumptions, namely:
 - short-lived gluinos decay very soon in the dump ($\tau < 10^{-11}$ s)
 - weakly interacting photinos survive to the dump and to the thick iron muon filters, and must be sufficiently long-lived to travel ~ 500 meters up to the detectors
 - the photino-nucleon cross-section (giving "anomalous neutral current" events), is model-dependent
 - due to the extremely small geometrical acceptance, the gluino and photino distribution at production may give non negligible factors; in particular the photino spectrum depends on the assumed hadronic decay products of the gluino.
- (ii) The limits given by the ARGUS collaboration [42] rely on the following predictions of ref. [43]: the $^3P_1 \chi_b$ state of bottomonium may decay into a $g\tilde{g}\tilde{g}$ final state with a branching ratio around 30%, if the gluino mass is lower than 5 GeV/c².
- (iii) The limits coming from ISR or Fermilab searches for long-lived particles [18-21] are rather assumption-independent.
- (iv) The limits given in the present experiment depend strongly on the R-hadron cross-section in the dump.

All results have been compared within the hypothesis of a gluino lifetime given by (4.4). All would be in trouble in the case of heavy photinos [30] or, of course, if $M_{\tilde{\gamma}} > M_{\tilde{g}}$.

From all the limits summarized in Fig. 7 we conclude that light R-hadrons containing gluinos with $M < 2 \text{ GeV}/c^2$ may be considered as experimentally excluded. Heavier gluinos are still allowed only for lifetimes between 10^{-16} s and 10^{-10} s for $M_{\tilde{g}} < 5 \text{ GeV}/c^2$, and for $\tau < 10^{-10} \text{ s}$ if $M_{\tilde{g}} > 5 \text{ GeV}/c^2$; this is a region which is difficult to explore experimentally [44]. The present experiment and previous results exclude gluinos with $\tau > 10^{-10} \text{ s}$ and masses up to $\sim 10 \text{ GeV}/c^2$. However, none of these experiments can exclude very long-lived gluinos ($\tau \gg 1 \text{ s}$) which have been considered in some models [45].

4.3 Consequences on heavy neutrinos

In the standard model of weak and electromagnetic interactions, neutrinos are considered as massless, and lepton numbers are separately conserved for each lepton family. But there is no fundamental prejudice to do so, and many models have considered the possible existence of massive neutrinos [46]. In most cases, the concept of flavour mixing is extended from quarks to leptons, and one defines an unitary matrix analogous to the Kobayashi-Maskawa matrix; therefore each weak flavour eigenstate ν_i is a linear combination of the mass eigenstates ν_j with mixing U_{ij} :

$$\nu_i = \sum_j \nu_j U_{ij} \quad \text{where } j \text{ runs over all mass eigenstates and } i = e, \mu, \tau \dots$$

The present experiment can detect only neutrinos heavy enough to decay into final states which may be $e^+e^-\nu$, $\mu^+\mu^-\nu$, π^+e^- , $\mu^+e^-\nu$, $\pi^+\mu^-$ for neutrinos, and the corresponding channels for anti-neutrinos. Such heavy neutrinos may be produced in rare decays of π and K mesons, or in semi-leptonic decays of charm (D and F) or beauty (B) mesons. In order to give quantitative limits, we have analyzed our results using the predictions of ref. 47:

- The branching ratio of F, D and B mesons into a heavy neutrino ν_j of mass M_{ν_j} , and a charged lepton i , is proportional to the mixing parameter (B.R. = $c |U_{ij}|^2$ with $c = 0.1$ to 10^{-3} , depending on the mass M_{ν_j});
- the branching ratio of heavy neutrinos into a final state containing a charged lepton ℓ is around 20% for $\ell^+\ell^-\nu$ decay, 50% for $\ell + \text{hadron}$ decay;
- the heavy neutrino decays with a lifetime which is given by:

$$\tau = \frac{a}{|U_{ij}|^2 (M_\nu)^N} \quad \text{with } N \sim 5 \text{ and } a \sim 5 \cdot 10^{-12} \text{ s}$$

this gives lifetimes corresponding to the sensitivity domain of the present experiment for $M_\nu < 2 \text{ GeV}/c^2$ and $|U_{ij}|^2 > 10^{-4}$.

The cross-section limits obtained in the above possible final states and lifetimes have been translated into regions excluded at 90% C.L. in the $|U_{ij}|^2, M_\nu$ plane; we have taken for the $D\bar{D}$ production cross-section the values given in the above sections.

The results are displayed on Fig. 8a for $|U_{ei}|^2$ and Fig. 8b for $|U_{\mu i}|^2$, and compared to limits previously published for $M_\nu > 100 \text{ MeV}/c^2$. A new domain of existence is excluded by the present experiment from $e^+e^-\nu$ or π^+e^- decays for $|U_{ei}|^2$, and from $\pi^+\mu^-$ decays for $|U_{\mu i}|^2$ and $M_\nu > 600 \text{ MeV}/c^2$. In the same M_ν range, previous results come essentially from neutrino beam dump experiments [48,49], which are sensitive to longer lifetimes and therefore smaller values of the mixing parameter (typically $|U|^2 < 10^{-4}$). Our results concerning $|U_{\mu i}|^2$ overlap partially with the recently published values from the CHARM wide band beam experiment [49], in which heavy neutrinos are supposed to be produced in a different way (via a flavour-changing neutral current interaction $\nu_\mu + \text{Nucleus} \rightarrow \nu_H + X$).

The combined results displayed in Fig. 8 restrict severely the existence of massive neutrinos up to masses around $15 \text{ GeV}/c^2$.

CONCLUSION

We do not see any evidence for the hadroproduction of new particles with mass in the range $1-10 \text{ GeV}/c^2$, decaying into at least 2 charged particles with lifetimes from $\sim 5 \cdot 10^{-11}$ to $\sim 5 \cdot 10^{-7} \text{ s}$. The limits on the cross-section times the branching ratio range from 0.3 to some hundreds of picobarns, depending on the lifetime; these limits are several orders of magnitude lower than previously given for not interacting particles with $\tau < 10^{-8} \text{ s}$. We have presented some consequences of these limits on the existence of several hypothetical particles such as heavy axion-like bosons, heavy neutrinos or gluinos. In particular, the present experiment excludes gluinos in a new range: roughly from 1 to 7 GeV/c^2 and lifetimes between 10^{-10} and 10^{-8} s , even assuming a substantial nuclear interaction cross-sections of the R-hadrons in which gluinos are embedded. These limits and those found by previous experiments, restrict severely the existence of gluinos lighter than $5 \text{ GeV}/c^2$ and exclude gluinos below $2 \text{ GeV}/c^2$.

ACKNOWLEDGEMENTS

Substantial modifications to the standard NA3 set-up have been ready on time for data taking 3 months only after the approval of the present experiment: we are indebted to the NA3 technical staff for this performance. We acknowledge gratefully the CERN SPS staff for the excellent beam conditions, Mr. M. Mur and Mrs. G. Rahal-Callot for the installation and operation of the 168/E emulator.

We gratefully acknowledge J. Ellis for several stimulating discussions on various aspects of supersymmetry and gluino physics.

APPENDIX

We give here indications on the simple way we have estimated the attenuation factor F coming from the heavy material of the beam dump.

Let us define the following quantities:

- L is the length of the beam dump, which is made of a heavy material of atomic number A and density d ;
- σ_p is the production cross-section of the studied particles X ,
 σ_o their interaction cross-section;
- λ_1 is the attenuation length of the incoming π^- beam in the dump material.

Let us consider now the interaction of one incoming particle X with a given nucleus; the particle is located at an abscissa x and has an impact parameter b with respect to the nucleus centre. The nuclear density is described by a continuous spatial distribution $\rho(x,b)$ with
 $A = \int \rho(x,b) dx d^2b$.

The interaction probability of the particle with impact parameter b is

$$p = 1 - \exp(-\sigma_o \int_{-\infty}^x \rho(y,b) dy)$$

Integrating over the whole nucleus volume, we get the number of interactions with the nucleus:

$$n = \int (1 - \exp(-\sigma_o T(b))) d^2b$$

$$\text{where } T(b) = \int_{-\infty}^{+\infty} \rho(y,b) dy$$

n may be conveniently written as:

$$n = \sigma_o A^\alpha \quad (A^\alpha \text{ being an "effective number" of nucleons.})$$

APPENDIX (Cont'd)

Defining λ_2 as the attenuation length (for X particles), coming from these interactions, we have

$$n = \frac{A}{\lambda_2 d N} = \sigma_o A^\alpha \quad (N = \text{Avogadro's number})$$

and therefore

$$\lambda_2 = \frac{A^{1-\alpha}}{\sigma_o d N}$$

with

$$\alpha = \frac{\text{Ln}\left(\frac{1}{\sigma_o} \int [1 - \exp(-\sigma_o T(b))] d^2b\right)}{\text{Ln}(A)}$$

\mathcal{L} being the luminosity of the experiment, the total number of outgoing X particles will be

$$N = \mathcal{L} \int_0^L \frac{1}{\lambda_1} \exp\left(\frac{-x}{\lambda_1}\right) \sigma_p \exp\left(-\frac{L-x}{\lambda_2}\right) dx$$

which after integration gives

$$N = \mathcal{L} \sigma_p \frac{\lambda_2}{\lambda_2 - \lambda_1} \left[\exp\left(\frac{-L}{\lambda_2}\right) - \exp\left(\frac{-L}{\lambda_1}\right) \right]$$

σ_p being the total number of initially produced X particles, we have therefore

$$F = \frac{\lambda_2 - \lambda_1}{\lambda_2 \left[\exp\left(-\frac{L}{\lambda_2}\right) - \exp\left(-\frac{L}{\lambda_1}\right) \right]}$$

To estimate λ_2 numerically, we take a Saxon-Woods representation of nuclear density with spherical distribution:

$$\rho(r) = \rho_o \frac{1}{1 + \exp\left(\frac{(r-a)}{c}\right)}$$

APPENDIX (Cont'd)

with $a = 1.14 A^{1/3}$ and $c = 0.545$ fm from Glauber and Matthiae [53].

λ_1 is taken from ref. 54 to be: $\sigma_1 = 11.7\text{cm}$ for 300 GeV/c π^- in tungsten ($A = 184$).

Finally, to obtain the values of F given in Table III, we give weights according to the luminosities corresponding to the dump lengths $L = 200\text{cm}$ and $L' = 220$ m used in the experiment.

REFERENCES

- [1] S. Dawson, E. Eichten and C. Quigg, Phys. Rev. D31 (1985) 1581
(preprint in 1983 : Fermilab Pub. 83/82-THY).
- [2] H. Haber and G.L. Kane, Phys. Reports 117c (1985) 2-4.
- [3] J.K. Yoh et al., Phys. Rev.Lett. 41 (1978) 684,
p-N production of the T at 300 GeV/c
J. Badier et al., Phys. Lett. 86B (1979) 98,
 π^- -N production of the T at 280 GeV/c.
- [4] J.G. Mc Ewen et al., Phys. Lett. 121B (1983) 198
J. Badier et al., Zeit Phys. C20 (1983) 101.
- [5] J. Badier et al., Nucl. Inst. Meth. 175 (1980) 319.
- [6] J. Badier et al., Proposal CERN/SPSC/P-197, March 1984 (unpublished)
J. Badier et al., Preprint CERN/EP 85-107 (unpublished).
- [7] S. Weisz, Thèse de troisième cycle, Université Paris XI, 1977
(unpublished).
- [8] Rev. of Particle Properties, Rev. of Mod. Physics 56 (1984).
- [9] J. Badier et al., Punch-through measurement on a 200 cm beam dump using
300 GeV incident pions - to be submitted to Nucl. Inst. and Meth.,
Jan. 1986.
- [10] R. Brun et al., Geant 2 Package, CERN/DD/05/86.
- [11] A. Kernan and G. van Dalen, Phys. Rep. 106C (1984) 298.
- [12] M. Aguilar-Benitez et al., Phys. Lett. 161B (1985) 400.
- [13] M.E. Duffy et al., Phys. Rev. Lett. 55 (1985) 1816.
- [14] See for instance V. Hagopian et al., Phys. Rev. Lett. 36 (1976) 296.
- [15] J. Badier et al., Phys. Lett. 39B (1972) 414.
- [16] M. Bourquin et al., Nucl. Phys. B 153 (1979) 13.
- [17] J.L. Thron et al., Phys. Rev. D31 (1985) 451.
- [18] R. Gustafson et al., Phys. Rev. Lett. 37 (1976) 474.
- [19] Fermilab. experiment D. Cutts et al., Phys. Rev. Lett. 41 (1978) 363
CERN SPS experiment A. Bussiére et al., Nucl. Phys. B 174 (1980) 1.
- [20] R. Vidal et al., Phys. Lett. 77B (1978) 344.
- [21] B. Alper et al., Phys. Lett. 46B (1973) 265
M. Albrow et al., Nucl. Phys. B114 (1976) 365.

REFERENCES (cont/d)

- [22] J.D. Bjorken, L.W. Mo et al., Fermilab Proposal E 635, 1980
(addendum in May 1982), (unpublished)
J.D. Bjorken, Proc. of Moriond Workshop on Massive Neutrinos,
p. 227, Ed. Frontiers, France, 1984.
- [23] T.W. Donnelly et al., Phys. Rev. D 18 (1978) 1607.
- [24] F. Bergsma et al., (CHARM Collaboration) Phys. Lett. 157B (1985) 458.
- [25] C. Edwards et al., Phys. Rev. Lett. 48 (1982) 903.
- [26] B. Niczyporuk et al., Z Phys. C 17 (1983) 197.
- [27] See for instance, among many review articles : H.P. Nilles,
Phys. Rep. 110C (1984) 1.
- [28] UA1 collaboration, G. Arnison et al., Phys. Lett. 139B (1984) 115.
- [29] E. Reya and D.P. Roy, Phys. Rev. Lett. 53 (1984) 881
J. Ellis and H. Kowalski, Phys. Lett. 142B (1984) 441
and many other recent references.
- [30] M.T. Herrero et al., Phys. Lett. 132B (1983) 199,
Phys. Lett. 145B (1984) 430
J. Berger et al., Phys. Rev. Lett. 53 (1984) 641.
- [31] R. Schwitters, concluding talk, International Symposium on Lepton and
Photon Interactions, Kyoto (Japan), August 1985.
- [32] P. Fayet, Phys. Lett. 64B (1976), 159,
Phys. Lett. 69B (1977), 489.
- [33] M. Chanowitz and S. Sharpe, Phys. Lett. 126B (1983) 225
A. Mitra and S. Ono, Zeit. für Physik C 25 (1984) 245.
- [34] F. Buccella, G. Farrar and A. Pugliese, Phys. Lett. 153B (1985) 331.
- [35] G.L. Kane and J.P. Leveille, Phys. Lett. 112B (1982) 227.
- [36] P.R. Harrison and C.H. Llewellyn Smith, Nucl. Phys. B 213 (1983) 223.
- [37] CHARM Collaboration, F. Bergsma et al., Phys. Lett. 121B (1983) 429.
- [38] E613 Collaboration, R.C. Ball et al., Phys. Rev. Lett. 53 (1984) 1314.
- [39] BEBC WA66 Collaboration, A.M. Cooper-Sarkar et al.,
Phys. Lett. 160B (1985) 212.

REFERENCES (Cont/d)

- [40] The WA75 Collaboration, J.P. Albanese et al.,
Phys. Lett. 158B (1985) 186, has seen 1 beauty event in
350 GeV $\pi^- p$ interactions, corresponding to $\sigma \sim 10$ nb;
The NA3 Collaboration, J. Badier et al., Phys. Lett. 124B (1983) 353
sets model-dependent upper limits from 2 to 5 ub/nucleon on beauty
production in 280 GeV π^- interactions.
- [41] NA3 Collaboration, J. Badier et al., Phys. Lett. 86B (1979) 98.
- [42] ARGUS Collaboration, H. Albrecht et al.,
DESY Internal Report, No 85-129 (Nov. 1985).
- [43] B.A. Campbell, J. Ellis and S. Rudaz, Nucl. Phys. B 198 (1982) 1.
- [44] A. de Rujula and E. Franco, Phys. Lett. 153B (1985) 183;
R. Petronzio and A. de Rujula, Nucl. Phys. B261 (1985) 587.
- [45] For instance, light gluinos ($M < 1$ GeV/c²) with very long lifetime
($\tau > 3$ years) have been invoked as a possible explanation of the
Cygnus X 3 signal:
G. Auremma, L. Maiani and S. Petrarca, Phys. Lett. 164B (1985) 179.
On the contrary, there are arguments to exclude gluinos with
 $M < 4$ GeV/c² and $\tau > 10^6$ s :
L.B. Okun and M.B. Voloshin, Preprint ITEP 85-119, Moscow (Nov. 1985).
- [46] For a list of references on heavy neutrinos, see for instance
Ref. 11 of :
C.N. Leung and J.L. Rosner, Phys. Rev. D28 (1983) 2205.
- [47] M. Gronau, C.N. Leung and J.L. Rosner, Phys. Rev. D29 (1984) 2539.
- [48] BEBC WA66 Collaboration, A. Cooper-Sarkar et al., Phys. Lett.
160B (1985) 207.
- [49] CHARM Collaboration : F. Bergsma et al., Phys. Lett. 128B (1983) 361;
J. Dorenbosch et al, Preprint CERN EP/85-190 (Nov. 1985).
- [50] PS 191 Collaboration : G. Bernardi et al., Preprint CERN EP/85-177
(Nov.1985).
- [51] MARK II Collaboration : G.J. Feldman, Preprint SLAC-PUB 3684, May 1985.
- [52] F.J. Gilman and S.H. Rhie, Phys. Rev. D32 (1985) 324.
- [53] R.J. Glauber and G. Matthiae, Preprint ISS 67/16, Istituto Superiore
di Sanità, Laboratori di Fisica, Roma (1967).
- [54] A.S. Carroll et al., Phys. Lett. 80B (1979) 319.

TABLE CAPTIONS

- Table I Number of events identified from their decay products, after applying the cuts described in the text. The mass reconstructed in the present experiment (with only statistical errors) is compared to the world average from Particle Data Group [8].
- Table II Number of reconstructed 2-body decay candidates (same cuts as in Table I, and cut on P_{out} described in the text), and highest invariant mass (in MeV/c^2) found in the quoted channel.
- Table III Correction factor to be applied to the cross-section limits given in Fig. 4 and 5, if the hypothetical particle considered interacts with the matter of the dump, with a given cross-section (see Appendix for the estimation of this factor).

TABLE I

channel	events	mean mass (MeV)	mass from [8] (MeV)
$K_S^0 \rightarrow \pi^+\pi^-$	223 372	$497.11 \pm .02$	$497.67 \pm .13$
$\Lambda \rightarrow p\pi^-$	13 937	$1115.75 \pm .03$	$1115.60 \pm .05$
$\bar{\Lambda} \rightarrow \bar{p}\pi^+$	3 190	$1116.10 \pm .07$	$1115.60 \pm .05$
$K^+ \rightarrow \pi^+\pi^+\pi^-$	1 714	$494.0 \pm .2$	$493.667 \pm .015$
$K^- \rightarrow \pi^+\pi^-\pi^-$	529	$493.9 \pm .3$	$493.667 \pm .015$
$\Xi^- \rightarrow \Lambda\pi^-$	197	$1322.5 \pm .5$	$1321.32 \pm .13$
$\bar{\Xi}^+ \rightarrow \bar{\Lambda}\pi^+$	74	$1322.1 \pm .7$	$1321.32 \pm .13$
$\gamma \rightarrow e^+e^-$	510	$6.5 \pm .1$	0

TABLE III

Interaction cross section	Increase in the σ_B limits
1 mb/nucleon	8.8
2 mb/nucleon	58
5 mb/nucleon	4500
10 mb/nucleon	$3.2 \cdot 10^5$
20 mb/nucleon	$7.0 \cdot 10^6$

TABLE II	
----------	--

e	616 376							<div>xxx = number of events xxx = highest mass (MeV)</div>
μ	29 394	1664 608						3π <div>2434 1061</div>
π	1390 609	11142 1016	210759 997					> 4π <div>1 1007</div>
K	0	0	31 1105	0				
p	0	151 1109	15036 1720	0	0			
K _S ⁰	0	0	83 1266	0	0	0		
Λ	0	0	297 1475	0	0	0	0	
	e	μ	π	K	p	K _S ⁰	Λ	

FIGURE CAPTIONS

Fig. 1 Experimental set-up of the NA3 spectrometer during the present experiment.

Fig. 2 Mass spectra (number of events for 10 MeV/c² mass bins) of some final states, with the cuts described in the text to isolate 2-body decays :

- a) $\pi^+\pi^-$ final state, with the $K^0_s \rightarrow \pi^+\pi^-$ peak with long tails extending well above the K^0_s mass, due to multiple scattering effects. The bump around 350 MeV/c² may come from $K_L^0 \rightarrow \pi^+\pi^-\pi^0$ when the π^0 is undetected.
- b) e^+e^- final state. The peak below 10 MeV/c² comes from e^+e^- pair creation by energetic photons in the walls of the vacuum tank.
- c) $\mu^+\mu^-$ final state.

Fig. 3 Mass spectra (number of events for 10 MeV/c² mass bins) of candidates for three-body decays :

- a) $\pi^+\pi^-$ final state, without cut selecting 2-body decays
- b) $\pi^+\pi^-\pi^\pm$ final state, with the K^\pm peak.

Fig. 4 Examples of 90% C.L. upper limits on cross section production, times branching ratio, σB , of neutral particles X^0 , function of the particle lifetime τ . σB is given in picobarns/nucleon, assuming no nuclear effect in the production, and negligible reinteraction in the dump

Curve a)	$X^0 \rightarrow e^+e^-$	$M_X = 100 \text{ MeV}/c^2$
b)	$X^0 \rightarrow \mu^+\mu^-$	$M_X = 600 \text{ MeV}/c^2$
c)	$X^0 \rightarrow \pi^+\pi^-$	$M_X = 5 \text{ GeV}/c^2$

FIGURE CAPTIONS (Cont'd)

Fig. 5 Contours of equal 90% C.L. upper limits on cross section times branching ratio (in picobarn/nucleon), in the Mass-Lifetime plot, assuming no nuclear effect in the production and negligible reinteraction in the dump

- a) $X^0 \rightarrow e^+\pi^-$
- b) $X^0 \rightarrow \mu^+\pi^-$ (the curves are almost the same for $X^0 \rightarrow \mu^+\mu^-\nu$)
- c) $X^0 \rightarrow \pi^+\pi^- + X'$
- d) $X^\pm \rightarrow \pi^+\pi^-\pi^\pm$.

Fig. 6 Values of axion-like mass M_x and decay constant F_x (in GeV) of axion-like particles excluded at 90% C.L. by the present experiment. Limits from previous works are taken from the results and compilations of the CHARM experiment (ref. 24), from which the figure elements have been taken.

Fig. 7 Exclusion of the existence of gluinos in the $(M_{\tilde{g}} - M_{\tilde{q}})$ plane. Full lines contours : regions excluded with 90% C.L. by the present experiment, supposing a gluino interaction cross section of respectively 0, 5, 10 and 20 millibarns.

Thin lines: curves of equal gluino lifetime, given by the expression

$$\tau(\tilde{g}) = 7.5 \cdot 10^{-20} (M_{\tilde{q}})^4 / (M_{\tilde{g}})^5$$

The regions enclosed inside dashed lines are excluded by previous experiments:

- CHARM [37], E613 [38], BEBC [39]
- ARGUS experiment [42]
- ISR and Fermilab experiments on long-lived particles [18-21].

FIGURE CAPTIONS (Cont'd)

Fig. 8 Exclusion of the existence of heavy neutrinos ν_H having a coupling $|U_{ej}|^2$ to electron neutrino (Fig. 8a), or $|U_{\mu j}|^2$ to muon neutrino (Fig. 8b), as a function of the neutrino mass M_ν ($|U_{ij}|^2$ should never attain values close to 1, due to the unitarity of the U-matrix).

Full lines contours: regions excluded with 90% C.L. limit by the present experiment, from $e^+e^-\nu$ or $\pi^\pm e^\mp$ final states (Fig. 8a) or $\pi^\pm \mu^\mp$ final states (Fig. 8b).

Dashed or dotted-line contours: regions excluded by previous experiments:

- BEBC: neutrino beam-dump experiment [48]
- CHARM: neutrino beam-dump and wide band beam experiments [49]
- PS191: best results from $K \rightarrow e\nu_H$ or $K \rightarrow \mu\nu_H$ decays [50]
- MARK II: limits obtained by the MARK II collaboration at PEP, assuming the reaction $e^+e^- \rightarrow \nu_H \bar{\nu}_H$ [51]
- PEP MONOJETS: limits derived in ref. 52 from PEP search for monojets coming from $e^+e^- \rightarrow \bar{\nu}_e \nu_H$

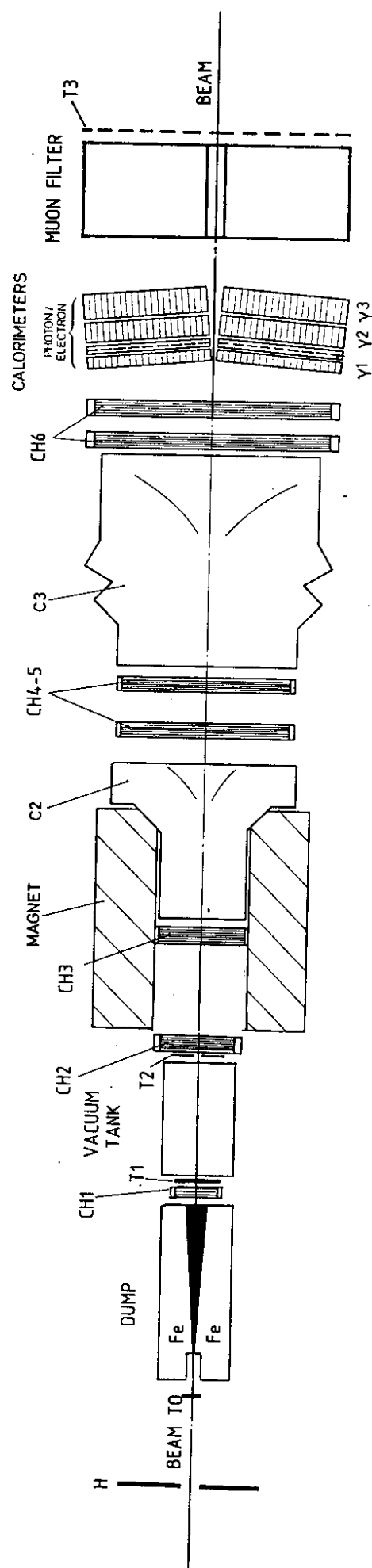


FIG. 1

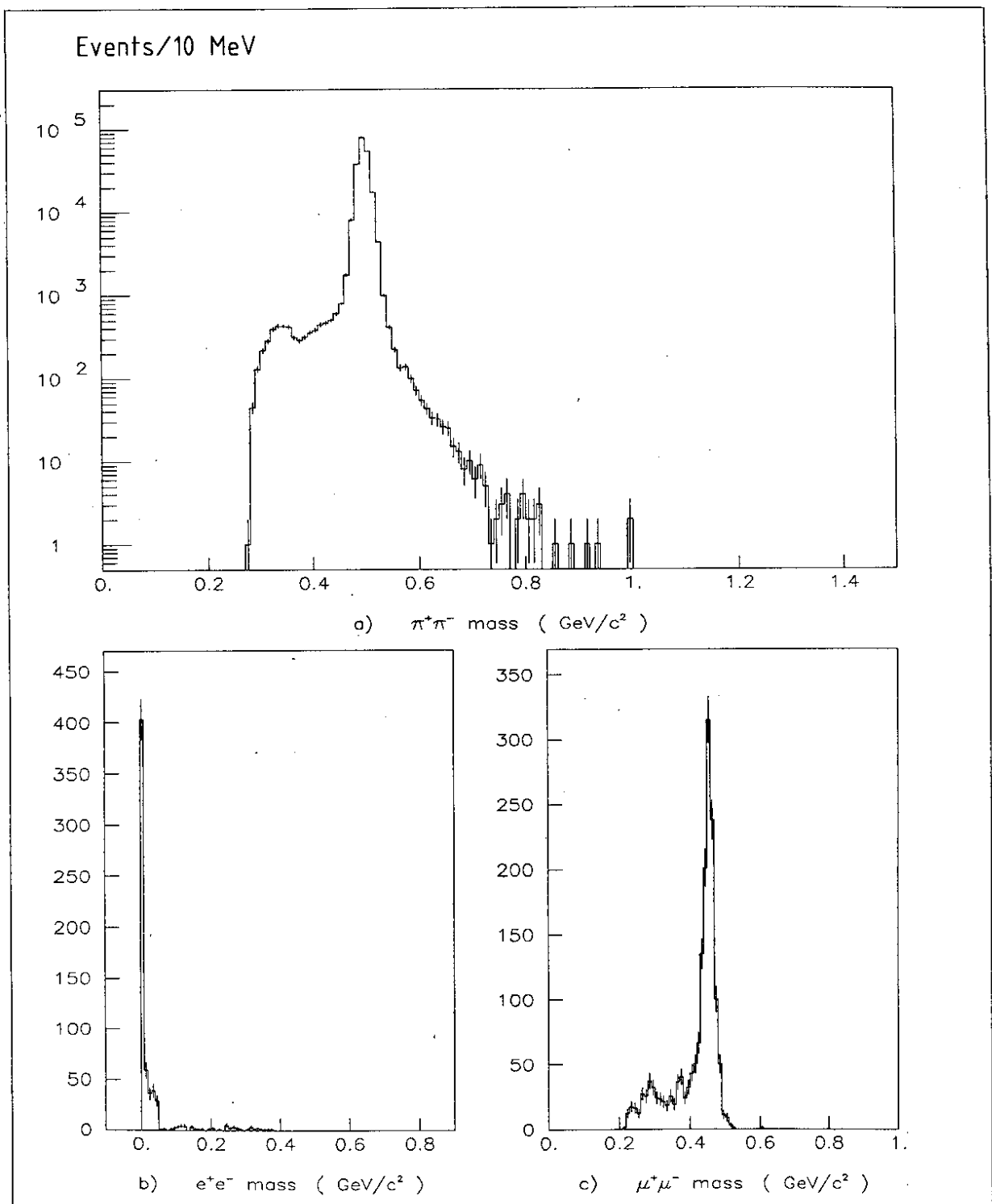


FIG. 2

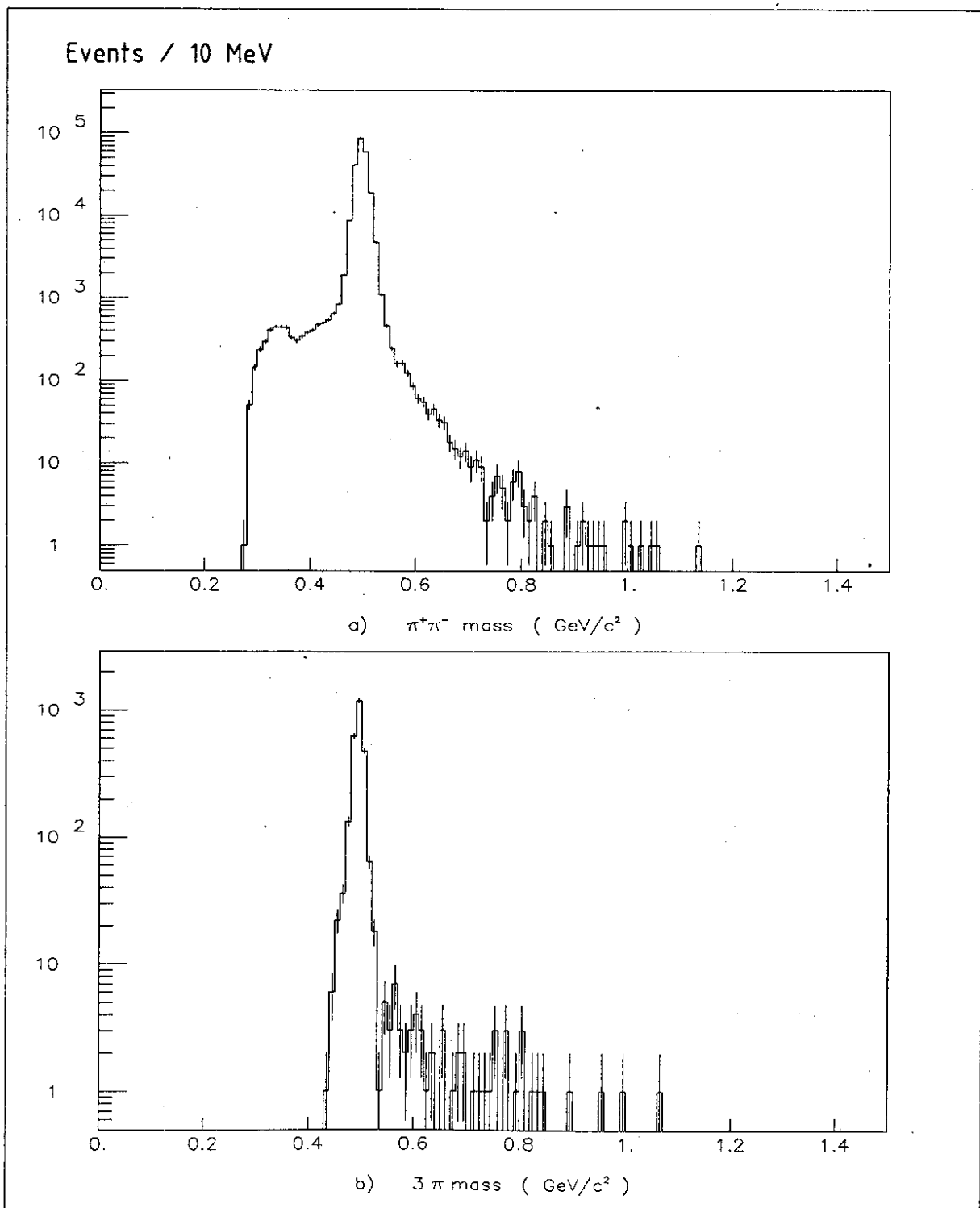


FIG. 3

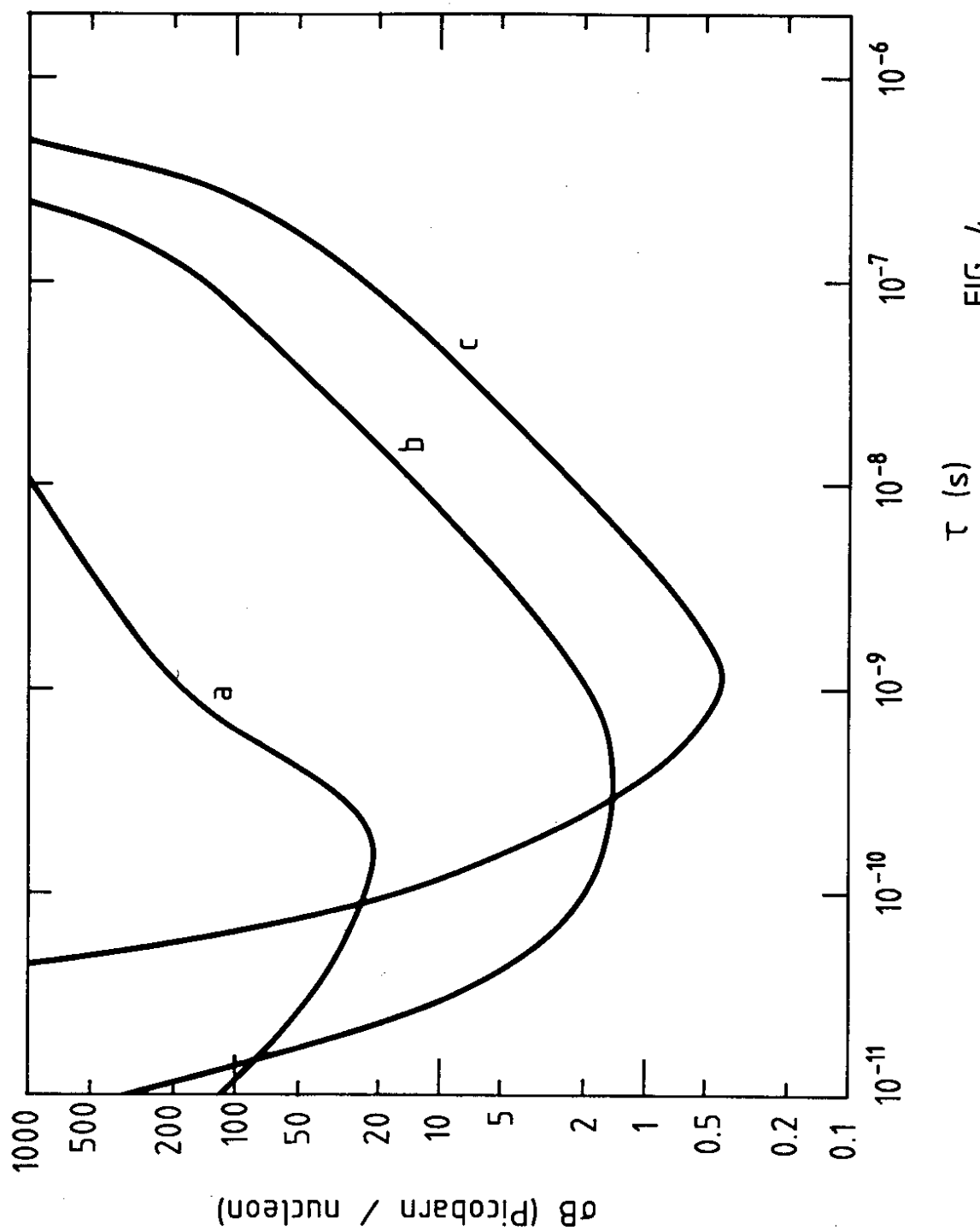


FIG. 4

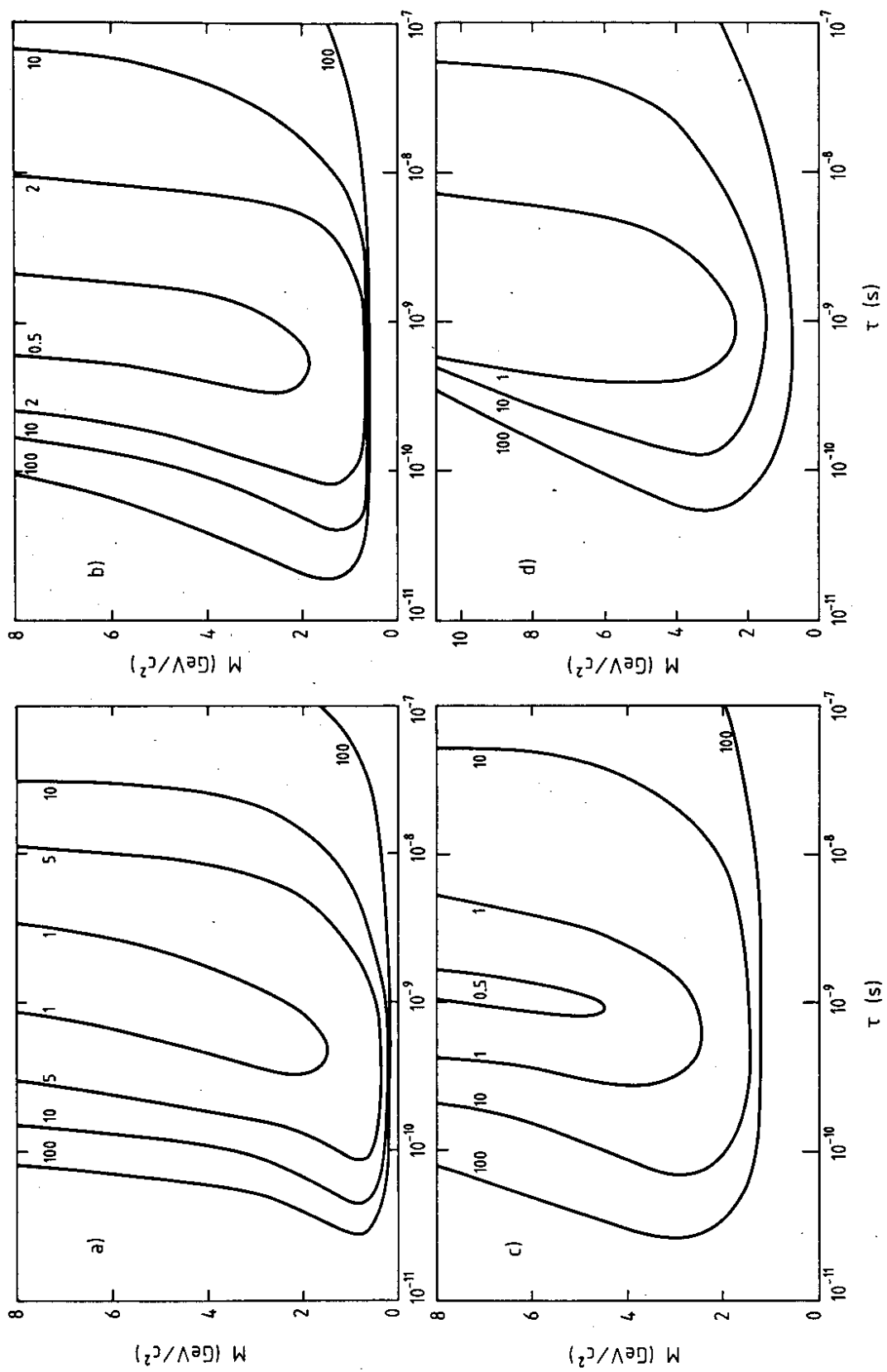


FIG. 5

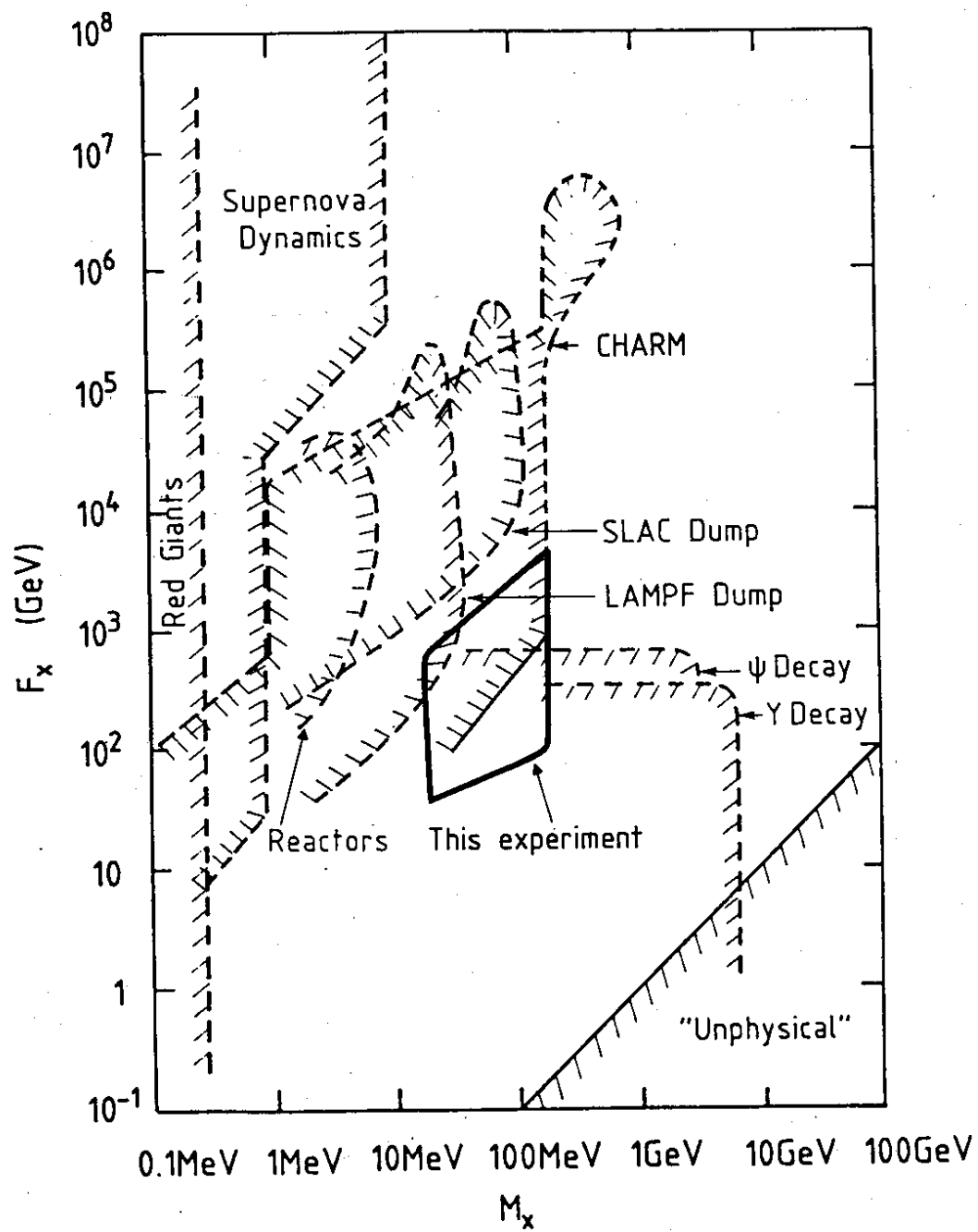


FIG. 6

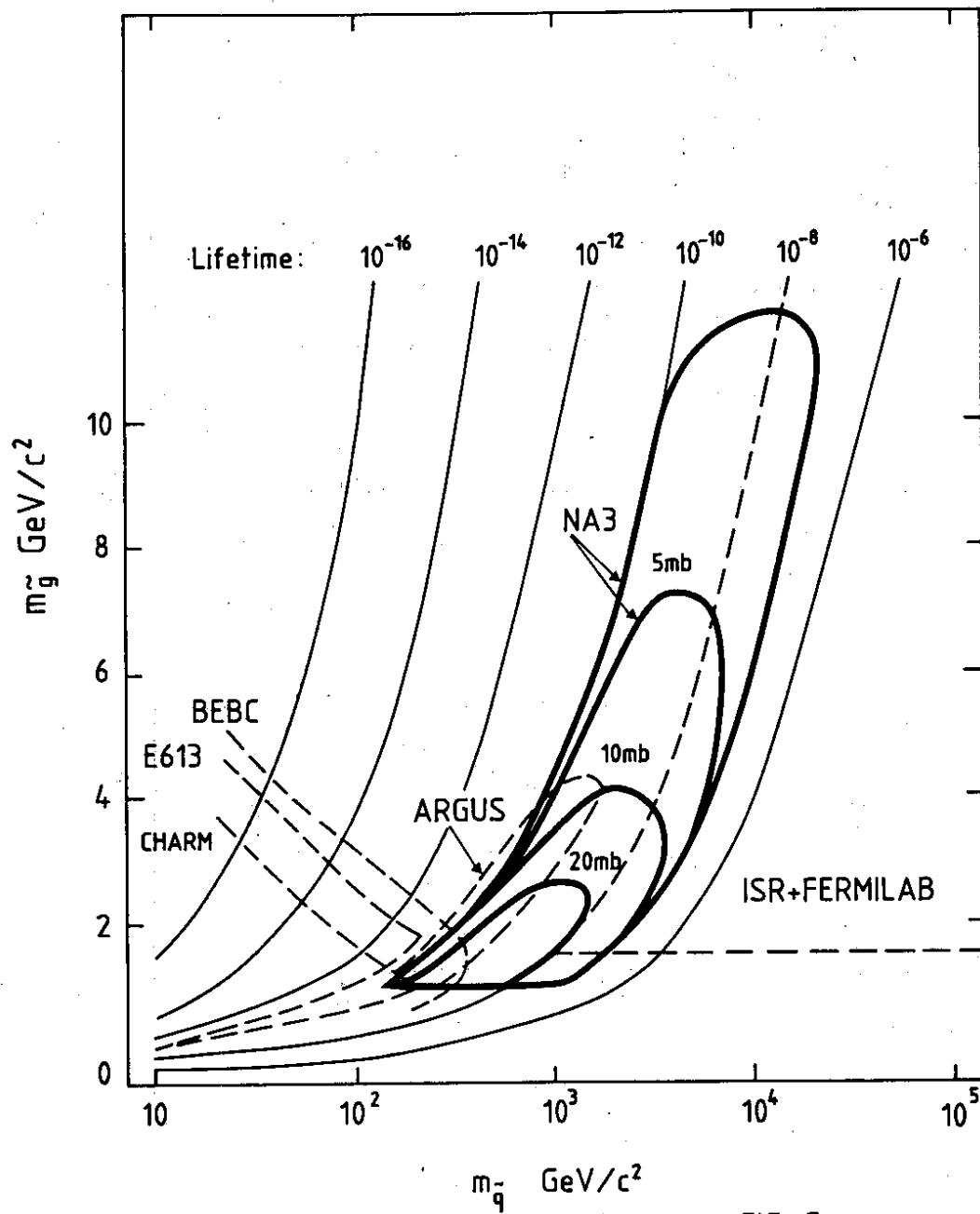


FIG. 7

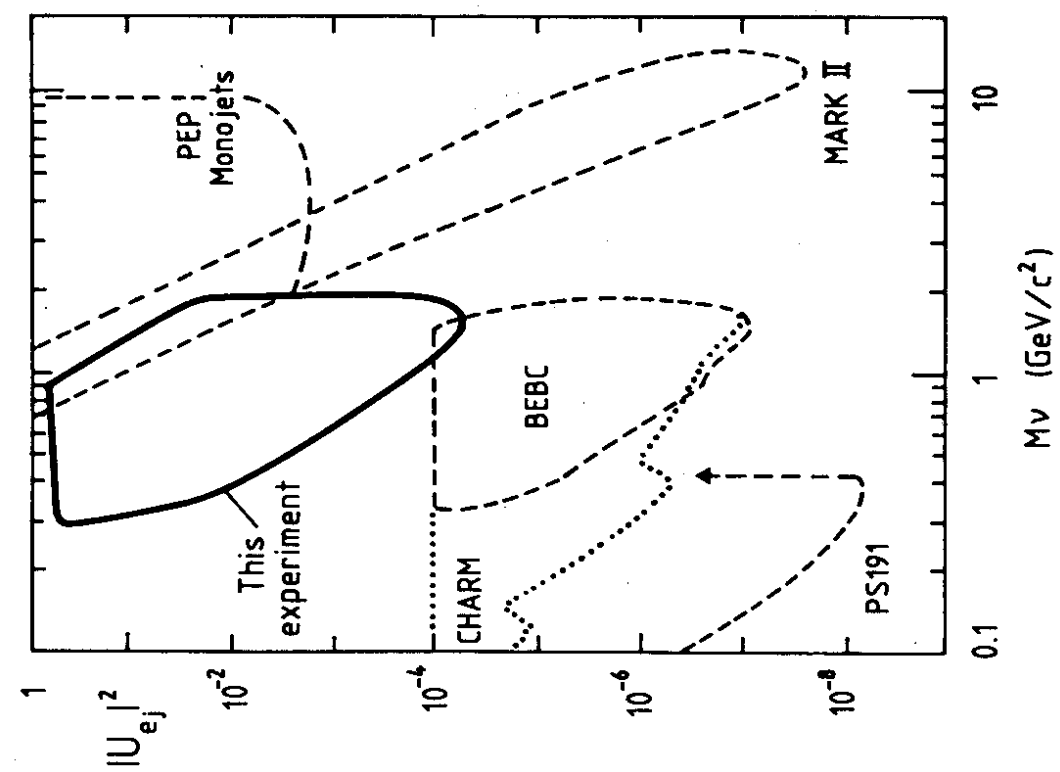


FIG. 8a

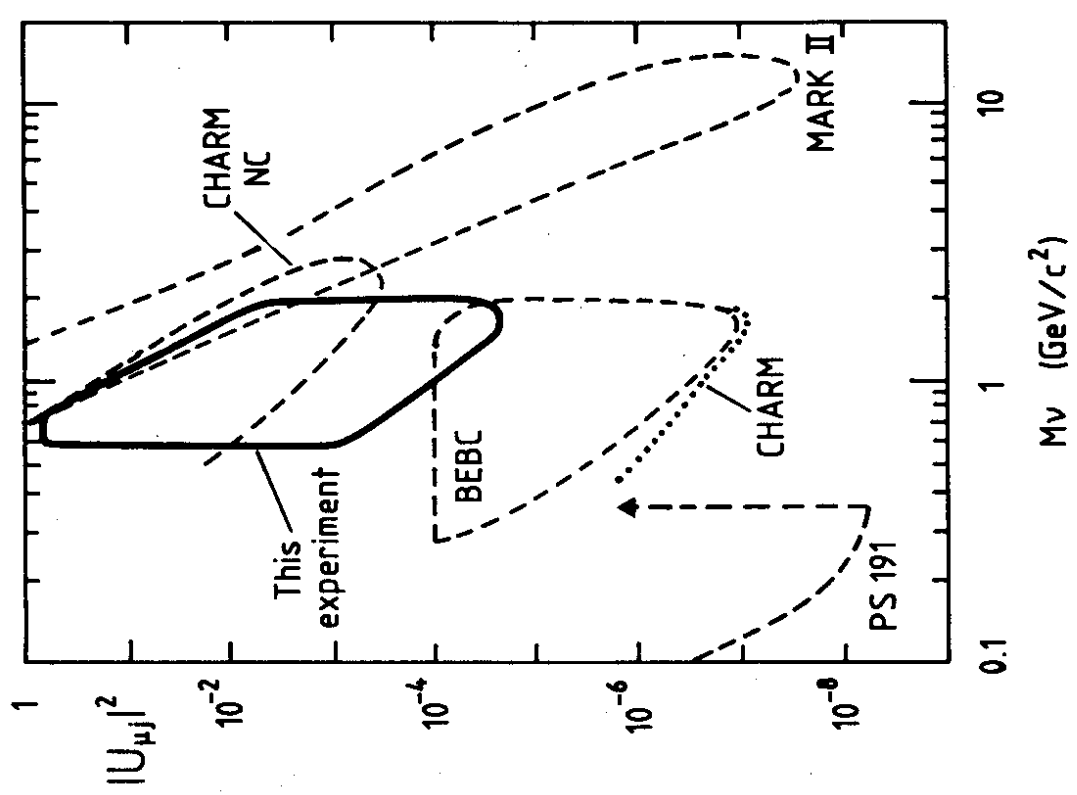


FIG. 8b